AMXTH-CD-TR-86058

(4)

STUB PENETRATION IN CHEMICAL MUNITION SHIPMENT

by
Peter S. Westine

FINAL REPORT
SwRI Project No. 06-8461-003 / 004

May 1985

DISTRIBUTION UNLIMITED / APPROVED FOR PUBLIC RELEASE

Prepared for

U.S. ARMY TOXIC AND HAZARDOUS MATERIALS AGENCY
ABERDEEN PROVING GROUND, MARYLAND 21010-5401

DISCLAIMER

The findings in this report are not to be construed as an official Department of the Army position unless so designated by other authorizing documents.

UNCLASSIFIED

SECURITY CLASSIFICATION OF THIS PAGE

REPORT DOCUMENTATION PAGE

1a. REPORT SECURITY CLASSIFICATION Unclassified	1b. RESTRICTIVE MARKINGS None AD-A189797
2a. SECURITY CLASSIFICATION AUTHORITY NA	3. DISTRIBUTION/AVAILABILITY OF REPORT Distribution Unlimited/Approved for Public Release AMCPEB-CD
2b. DECLASSIFICATION/DOWNGRADING SCHEDULE NA	
4. PERFORMING ORGANIZATION REPORT NUMBER(S) 06-8461-003/004	5. MONITORING ORGANIZATION REPORT NUMBER(S) AMXTH-CD-TR-86058 Chemical Demilitarization
6a. NAME OF PERFORMING ORGANIZATION Southwest Research Institute 6b. OFFICE SYMBOL (If applicable)	7a. NAME OF MONITORING ORGANIZATION U.S. Army Toxic and Hazardous Materials Agency
6c. ADDRESS (City, State, and ZIP Code) P. O. Drawer 28510 6220 Culebra Road San Antonio, Texas 78284	7b. ADDRESS (City, State, and ZIP Code) Aberdeen Proving Ground, MD 21010-5401
8a. NAME OF FUNDING/SPONSORING ORGANIZATION H&R Technical Associates, Inc. 8b. OFFICE SYMBOL (If applicable)	9. PROCUREMENT INSTRUMENT IDENTIFICATION NUMBER
8c. ADDRESS (City, State, and ZIP Code) P. O. Box 215 Oak Ridge, Tennessee 37831	10. SOURCE OF FUNDING NUMBERS PROGRAM ELEMENT NO. / PROJECT NO. / TASK NO. / WORK UNIT ACCESSION NO.

11. TITLE (Include Security Classification)
Stub Penetration in Chemical Munition Shipment

12. PERSONAL AUTHOR(S)
Westine, Peter S.

13a. TYPE OF REPORT	13b. TIME COVERED	14. DATE OF REPORT (Year, Month, Day)	15. PAGE COUNT
Final	FROM _____ TO _____	85.05	24

16. SUPPLEMENTARY NOTATION

17 COSATI CODES			18. SUBJECT TERMS (Continue on reverse if necessary and identify by block number)
FIELD	GROUP	SUB-GROUP	
15	02		Transportation Accident, Stub Penetration, Chemical Munition Container, M55

19. ABSTRACT (Continue on reverse if necessary and identify by block number)

The M55 warhead carries a chemical agent which must be protected from accidental puncture in a shipment or handling accident. This report presents results from computer runs calculating the threshold impact velocity if a pallet of munitions or a protective package containing several pallets were to be dropped onto rigid stubs of different radii. Calculations were made for three separate cases. Case 1 involved stub penetration of a fiberglass shipping container and then the aluminum walls of the round. Case 2 added an extra layer of protection so that wooden two by fours had to be penetrated before the shipping container and munition walls were penetrated. Case 3 was an independent scenario involving puncture of a CAMPACT shipping container loaded on a flat bed railroad car or highway vehicle.

The computer code used to make all computation is a dynamic plasticity, multi-penetration stage, one just developed by SwRI for the U. S. Army Tank Automotive Command. Some comparisons are presented in which this code predicts experimentally observed penetrations to demonstrate the validity of its use in this study.

20. DISTRIBUTION/AVAILABILITY OF ABSTRACT	21. ABSTRACT SECURITY CLASSIFICATION
☐ UNCLASSIFIED/UNLIMITED ☒ SAME AS RPT. ☐ DTIC USERS	Unclassified
22a. NAME OF RESPONSIBLE INDIVIDUAL CPT Kevin J. Flamm	22b. TELEPHONE (Include Area Code) (301) 671-2424 22c. OFFICE SYMBOL AMXTH-CD-L

DD FORM 1473, 84 MAR 83 APR edition may be used until exhausted
All other editions are obsolete

SECURITY CLASSIFICATION OF THIS PAGE

UNCLASSIFIED

SOUTHWEST RESEARCH INSTITUTE
Post Office Drawer 28510, 6220 Culebra Road
San Antonio, Texas 78284

STUB PENETRATION IN CHEMICAL MUNITION SHIPMENT

by
Peter S. Westine

FINAL REPORT
SwRI Project No. 06-8461-003/004

for
H & R Technical Associates, Inc.
Oak Ridge, Tennessee

May 1985

Approved:

Alex B. Wenzel

Alex B. Wenzel, Director
Department of Energetic Systems

TABLE OF CONTENTS

LIST OF FIGURES

ACKNOWLEDGEMENTS

Ms. Donna O'Kelley and Mr. Patrick Zabel ran the computer program for all of the cases required in putting together this analysis. Ms. Rosemary Rivas typed this report and Mr. Victor Hernandez drew all figures. The cooperation of these individuals is appreciated.

STUB PENETRATION IN CHEMICAL MUNITION SHIPMENT

by

Peter S. Westine

Introduction

The M55 warhead carries a chemical agent which must be protected from accidental puncture in a shipment or handling mishap. In this project, computer runs were made to calculate the threshold impact velocity if a pallet of munitions or a protective package containing several pallets were to be dropped onto rigid stubs of different radii. Figure 1 shows schematically the M55 pallet with 15 rounds each inside a shipping/launching tube. The shipping tubes are made of fiberglass; therefore, if contacted from above or below, both the fiberglass container and the aluminum walls of the round must be penetrated before any chemical agent leakage can occur. Figure 2 presents the cross sections which must be penetrated for leakage to occur under these conditions, which shall be called Case 1. The total weight of one pallet with its fifteen rockets is 1350 lb.

Should the pallet in Figure 1 rotate so that the impact is on the side of a pallet, extra protection is provided by wooden two-by-fours in the pallet side walls. Thus, the Case 2 penetration analysis is for the threshold impact velocity to just penetrate a composite of wood, fiberglass, and aluminum when the pallet is dropped onto rigid stubs of different radii. The pallets being dropped in Cases 1 and 2 are identical. Only the pallet orientation and number of layers to be penetrated change.

The third accident scenario, Case 3, is puncture of a shipping container which might be loaded on a flat bed railroad car or highway vehicle. These protective packages are complex containers within a container. The one shown schematically in Figure 3 and analyzed in this study is called the CAMPACT. Many pallets of munitions would be stored in a CAMPACT shipping container; however, in Case 3 we only determine the threshold velocity for just penetrating a CAMPACT dropped onto different radii stubs. Thus, Case 3 does not include penetration of a loaded CAMPACT container plus pallets of munitions; however, as a first approximation, the threshold velocity for a pallet inside the CAMPACT is the square root of the sum of the velocities

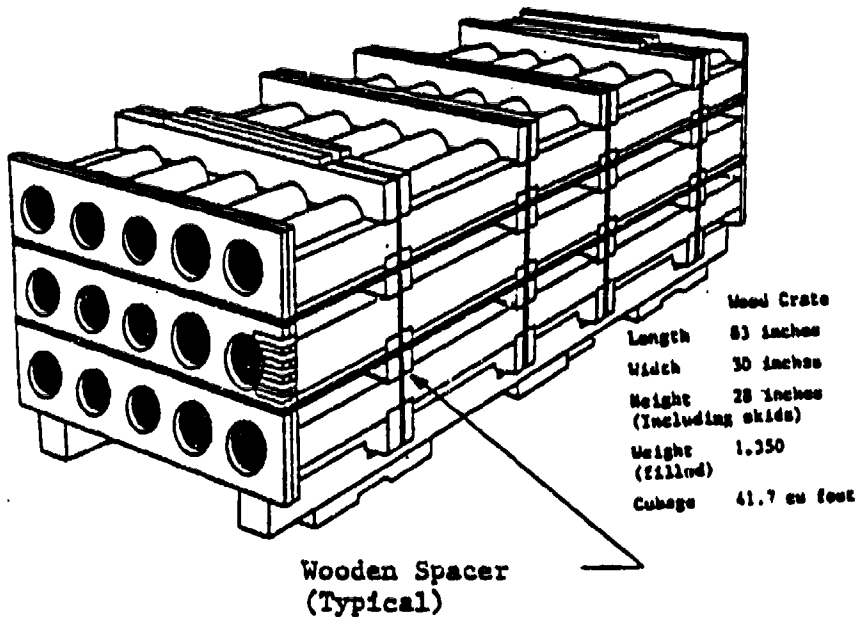

Figure 1. Pallet of M55 Missiles (in Launch Tubes)

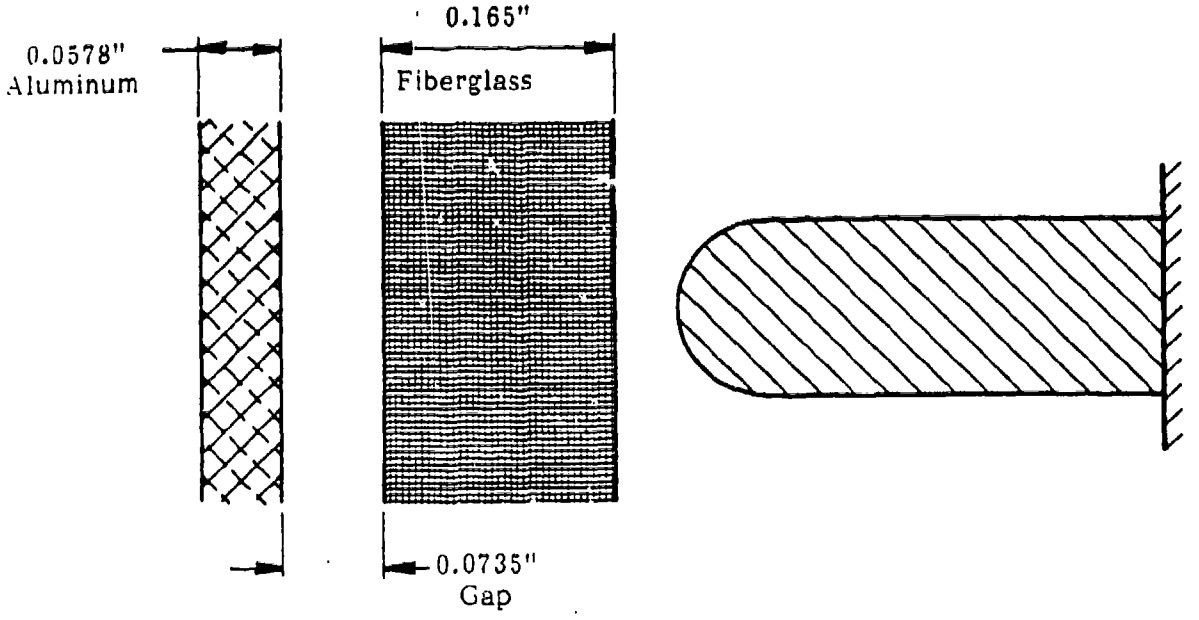

6061-T6

ρ = 0.100 lb/in.^{3}

σ_o = 40,000 psi

ε_{ult} = 0.14 in./in.

ρ = 0.0525 lb/in.^{3}

σ_o = 13,000 lb/in.^{2}

ε_{ult} = 0.014 in./in.

Total Weight of Pallet and Rockets 1,350 lb

Figure 2. Penetration Conditions in Case 1

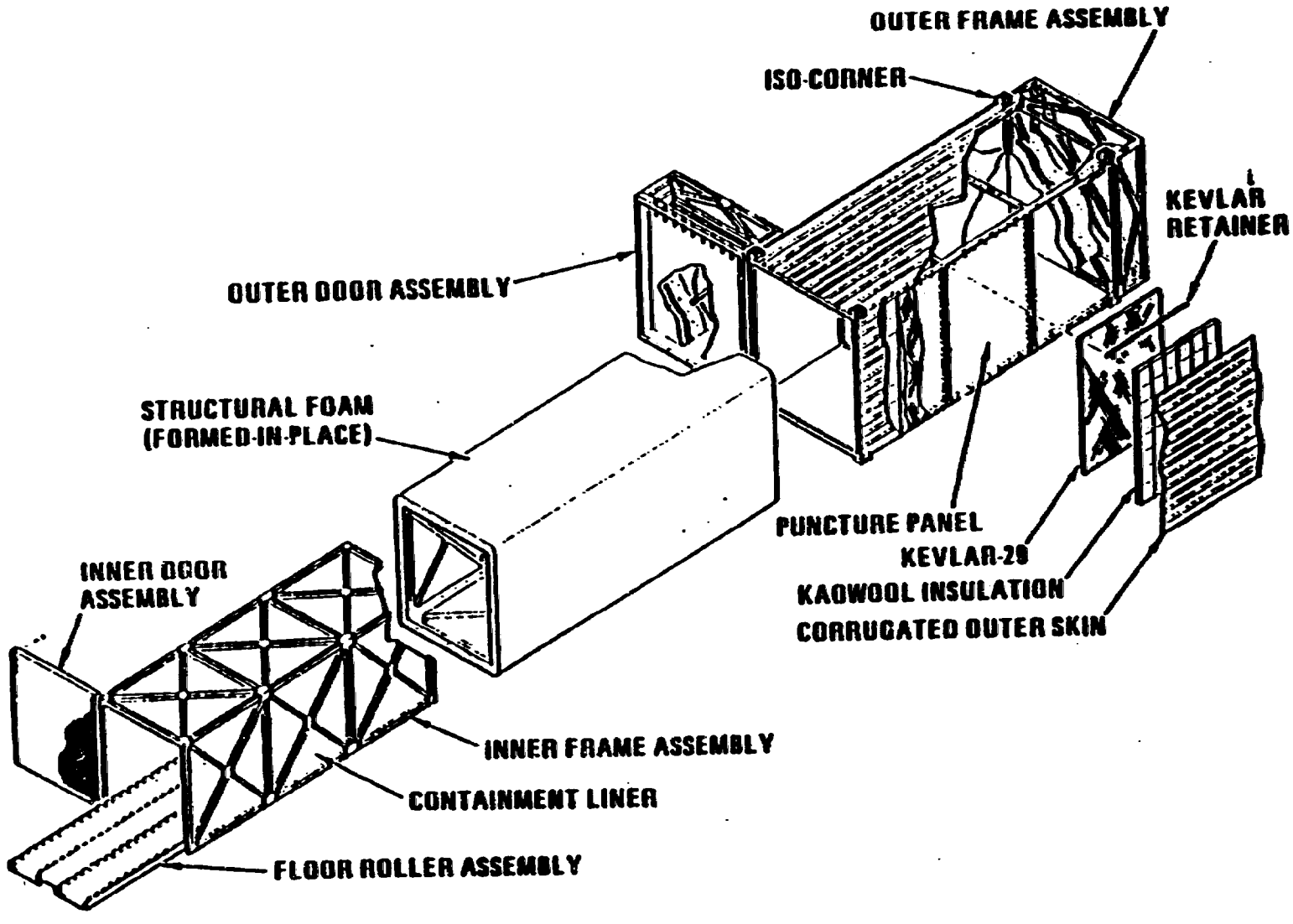

Figure 3. CAMPACT Construction Features

squared for Case 1 (or 2) and Case 3. A CAMPACT fully loaded with eight pallets weighs approximately 46,100 lb.

A cross-section through the walls of a CAMPACT is seen in the top-half of Figure 4. Many of the layers may as well not exist for puncture analysis. The steel skins surrounding the polyurethane foam are basically barriers for containing the foam when it is foamed in place after the inner and outer CAMPACT containers are assembled. The outer steel sheet is actually corrugated, but it is only 12 mils thick and is used for keeping out rain. Kaowool insulation, a very weak structural material, is a light, thermal insulation layer installed to protect the container contents from fire. For all practical purposes, the major anti-penetration armor is the Kevlar as our computations establish. The polyurethane foam was included in the analysis because it contributed a small amount of resistance due to its large thickness. The actual Case 3 cross-section studied computationally is that seen in the bottom half of Figure 4.

In this report, we will first present the results obtained from our calculations. A SwRI penetration code under development for the U.S. Army Tank Automotive Command called "Westine Eight-Stage Bodner Type Penetration Model" was used in all calculations. Details of how this code functions physically are described later in this report.

Results

Figure 5 is a plot of the critical threshold penetration velocity V_{cr} versus stub radius R for Cases 1 and 2, for penetration of the M55 chemical munition in a pallet as in Figure 1. Failure occurs when the stub punches through the aluminum wall so that agent could leak out.

Two curves are seen in Figure 5. The lower curve is for Case 1 penetration as sketched in Figure 2 without any wooden crate between the shipping tubes and the stub. The upper curve is for the Case 2 penetration, penetration first of a soft pine two-by-four, followed by penetration of the fiberglass shipping tube plus aluminum wall of the munition. Properties for the two-by-four were assumed to be a weight density of 0.0126 lb/in^3 (21.8 lb/ft^3), a flow stress of 1800 psi, and an ultimate strain of 0.04 in/in. Woods vary greatly in material properties even among the same species. Where the wood was taken from in a tree, whether grains are close together or far apart, etc., all influence mechanical properties. These particular values

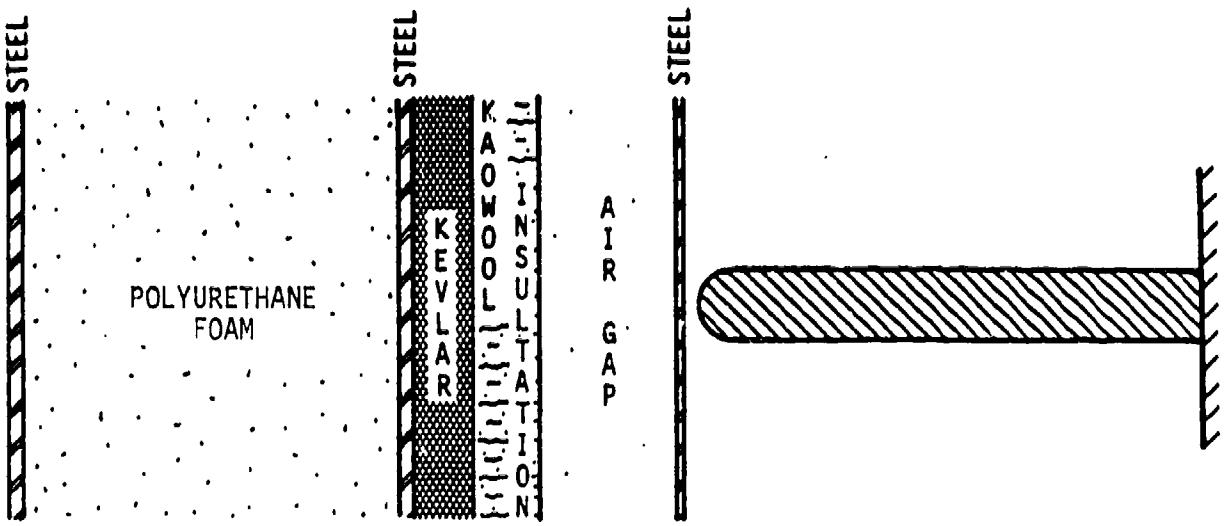

ρ = 0.00361 lb/in.^{3}

σ = 100 psi

ε_{ult} = 0.10 in./in.

H = 7.50 in.

ρ = 0.0521 lb/in.^{3}

σ = 50,000 psi

ε = 0.035 in./in.

H = 0.843 in.

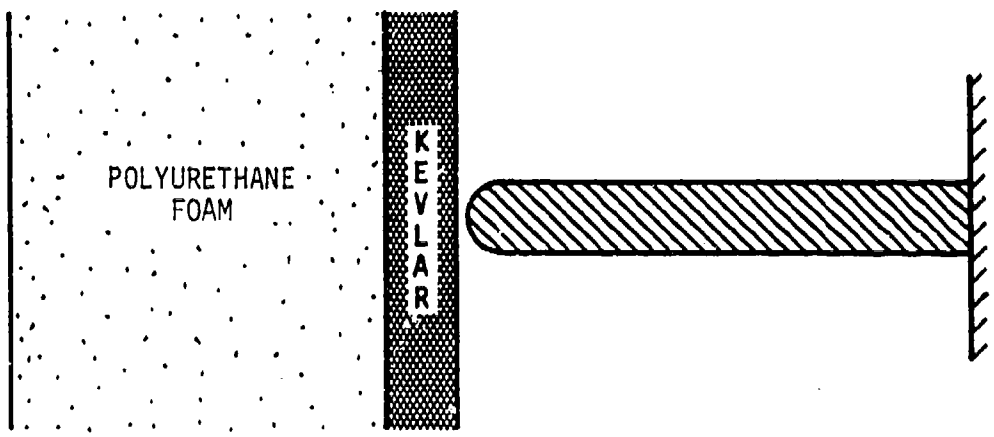

Total weight of fully loaded CAMPACT is 46,100 lbs.

Figure 4. Penetration Conditions for Case 3

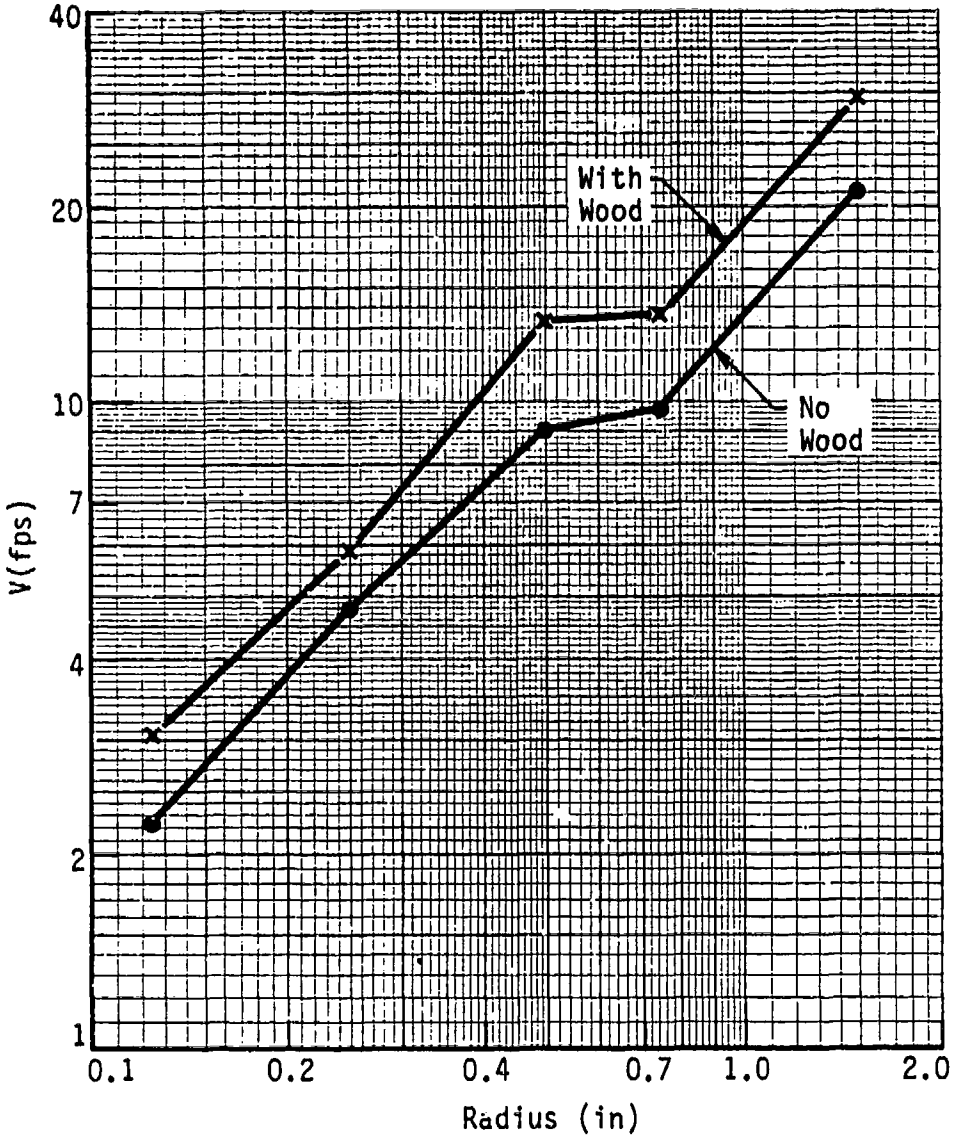

Figure 5. Threshold of Penetrating A Crate of Munitions

were selected as being representative of a weak pine. A weak pine, rather than a wood with stronger properties, was used so the calculation would be conservative. In all of these computations, the stub is treated as long and rigid.

As has already been described, the third case is penetation of a CAMPACT shipping container. Figure 6 is a plot of threshold penetration velocity versus stub radius for threshold of penetration into the 46,100 lb fully loaded CAMPACT container. In some studies, the resistance of the CAMPACT to puncture has been studied by remaking the container into an equivalent thickness of mild steel. This approach is not one which we favor because the equivalent thickness changes with stub radius as well as mode of response. Nevertheless, we did make calculations for equivalent threshold mild steel thickness.

After specific values for CAMPACT threshold penetration velocity onto different radii stubs had been obtained, each of the velocity and radius combinations was used in the same computer program to determine the thickness of rolled homogeneous mild (1020) steel that would just defeat each impact combination. The steel was assumed to be 1020 cold-rolled with a flow stress of 56,000 psi, a weight density of 0.283 lb/in^3, and an ultimate strain of 0.15 in/in. Also plotted in Figure 6 is the equivalent thickness of a 1020 mild steel armor. These thicknesses change with stub radii. With different physical processes taking on other relative importance as target thickness and material properties change, use of the equivalent armor concept is questionable as the same physical processes are not always being studied. We recommend using the lower curve in Figure 6 directly whenever system assessments are conducted.

Computer Code Validation

To demonstrate that this code can properly handle stub penetration into objects at low velocities of impact, two types of comparisons were made. In the first, we went to the literature and gathered a large quantity of test data obtained by Spaller* in 1966. In one series, of experiments Spaller drop-tested blocks of lead onto stubs of different diameters. Different

*A. E. Spaller, Structural Analysis of Shipping Casks, Vol. 2 Resistance to Puncture, September 1966, ORNL TM 1312.

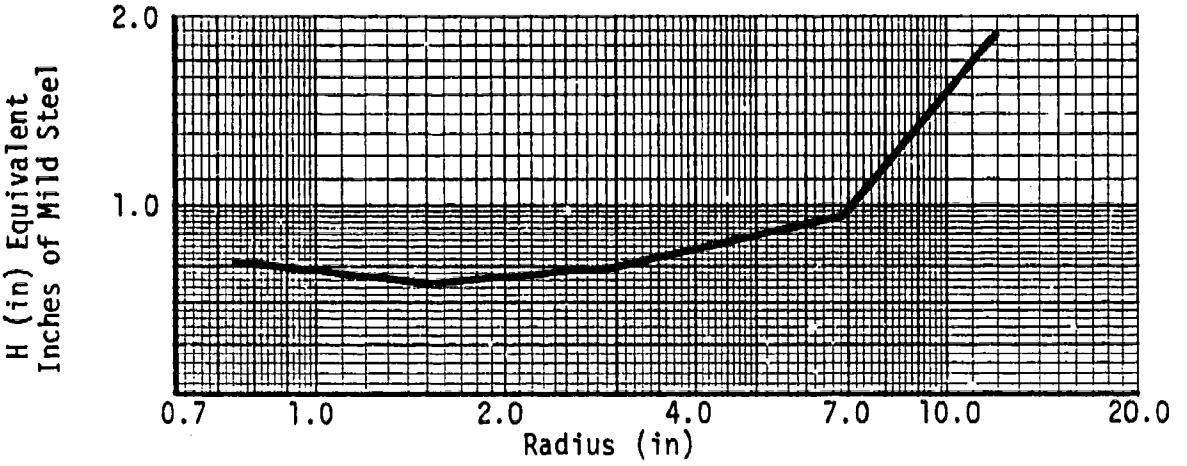

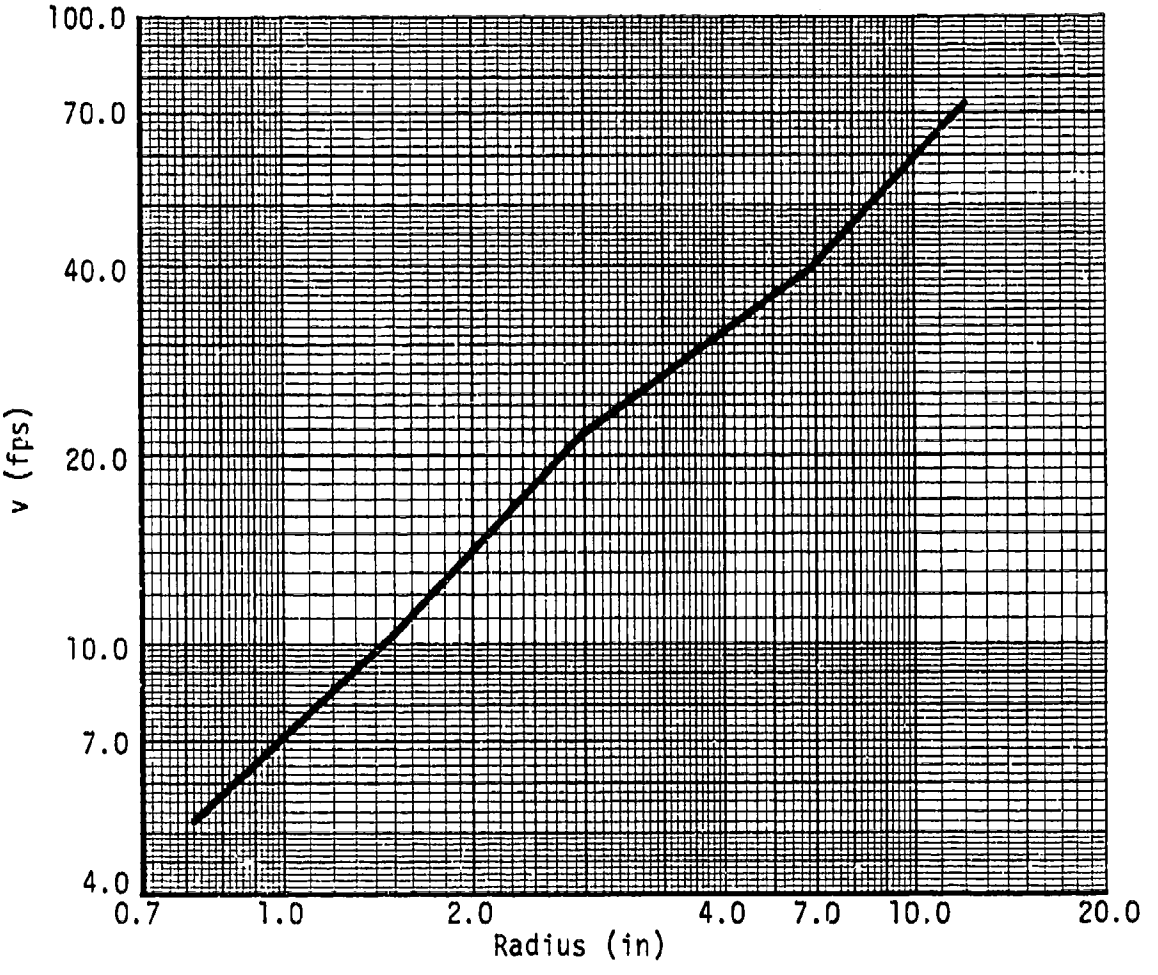

Figure 6. Threshold of Penetrating CAMPACT

weights of lead blocks were drop-tested (either 26, 52, 78, or 104 pound weights) on various diameter stubs (either 3/8, 1/2, or 5/8 inch diameter). Velocity of impacts ranged from 6.7 to 15.4 ft/sec for 52 pound weights. The recorded response for different impact velocities was depth of stub penetration into the lead. Figure 7 shows Spaller's test results plotted nondimensionally as scaled depth of penetration in stub diameters Y/d versus scaled energy of impact $E/\sigma_{ult}d^3$. By scaling the test results all can be presented on a single graph. The ultimate for the lead was 17,550 psi and the weight density was 0.411 lb/in^3. Because lead is ductile, the flow stress is lower closer to the yield point. The solid line in Figure 7 was calculated using the computer code used in this study with a flow stress of 6,800 psi for lead. Our purpose in making this run for this simplified case was to demonstrate that fairly accurate results can be obtained using this analysis procedure for homogeneous material penetrations.

The second comparisons to be made are for penetration into Kevlar. Kevlar is made by bonding together fine fibers. Such a material is not homogeneous. Parallel and perpendicular to the fibers, Kevlar has very different tensile as well as compressive ultimate strengths. Kevlar 29 fibers in tension have an ultimate strength of approximately 400,000 psi. In compression parallel to the fibers, it will have an ultimate strength of approximately 76,000 psi, and perpendicular to the fibers, an ultimate strength of approximately 38,000 psi. Some of these discrepancies are caused by different penetration processes occurring. When loaded across fibers, some failures are associated with fiber separation and spreading rather than a tensile tearing of fibers. The computer code that we used is currently designed to predict the response of homogeneous not heterogeneous materials. A representative flow stress of 50,000 psi was used for Kevlar, but its use needed validation. Large amounts of unclassified penetration data into Kevlar is unavailable; however, three data points were founded.

The designers of CAMPACT* describe a one-quarter scale replica model test designed to meet the intent of 10CFR71.73. Failure energy in this one-quarter scale model was 6,900 ft-lb. Because this model weighed 720 lb. this energy implies that the threshold velocity of impact in this model was 24.8 ft/sec.

---

*Information communication with Robert M. Burgoyne, G. A. Technologies, Inc., December 1984.

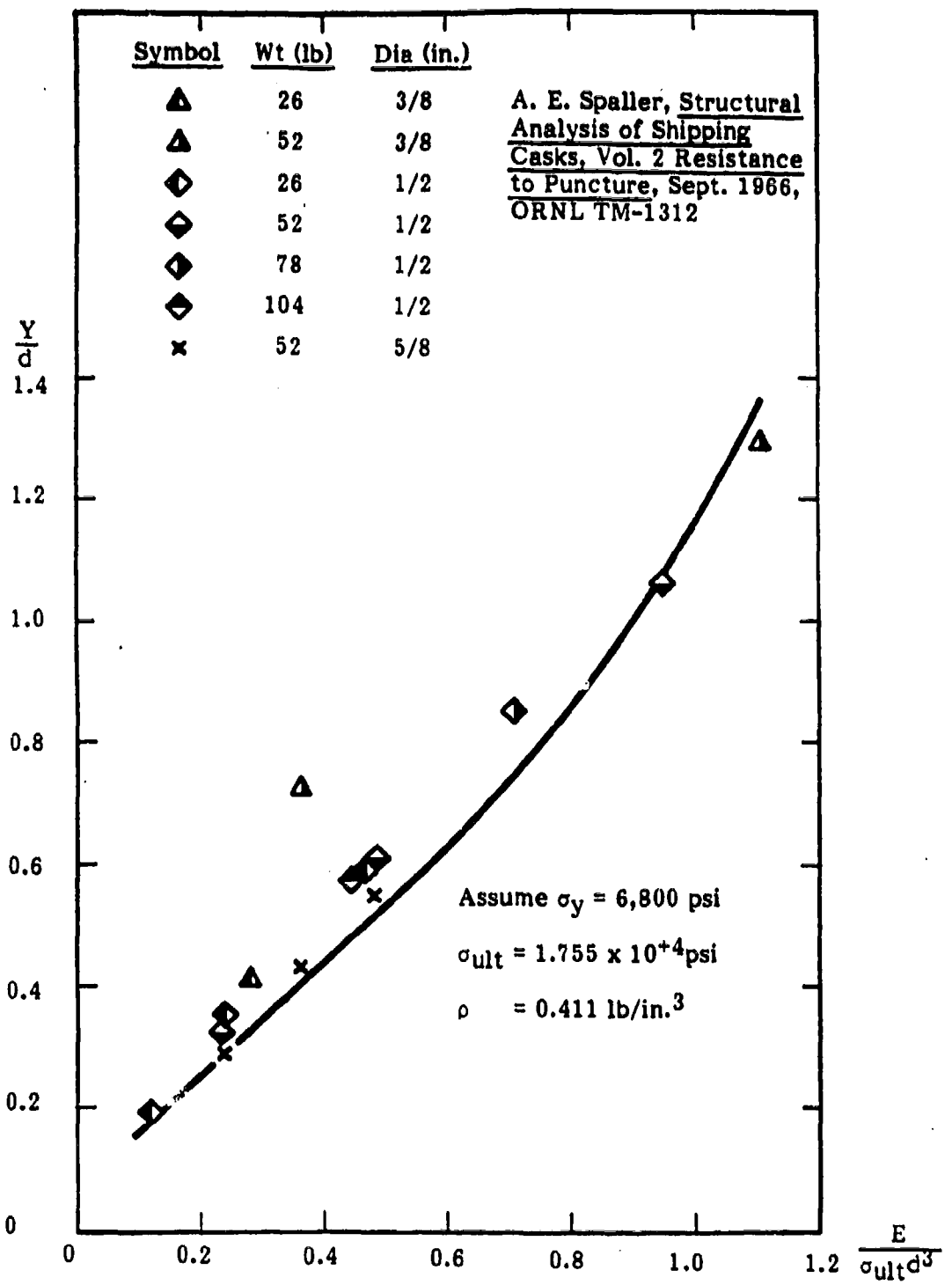

Figure 7. Penetration of Lead Blocks Dropped on Punch

Our computer code run predicted a threshold impact velocity of 25.1 ft/sec when the flow stress equaled 50,000 psi. This comparison indicated that a reasonable value was being used for flow stress, but one point comparisons can be fortuitous.

Other Kevlar penetration data were furnished by the U.S. Army Mechanics and Materials Research Center, Watertown, Massachusetts.* Figures 8 and 9 present unclassified ballistic limit data for 5.56 mm and 7.62 mm ball ammunition fired into Kevlar panels. The 5.56 mm ball projectile associated with results in Figure 8 weighs 0.00766 lb. At an initial impact velocity of 2400 fps, we calculated the ballistic limit thickness to be 0.683 inches. This value is essentially the same as that shown in Figure 8. The 7.62 mm ball projectile associated with results presented in Figure 9 weighs 0.02167 lb. At a muzzle velocity of 2740 fps as shown in Figure 9, we calculated a ballistic limit thickness of 1.38 inches. This too is essentially the same as was observed empirically. The predictive consistency in these three Kevlar comparisons indicate that a flow stress of 50,000 psi is a realistic value for Kevlar 29.

Computer Code Discussion

The computer code used in this analysis is a new one under preparation by SwRI for the U.S. Army Tank-Automotive Command, Warren, Michigan. The approach being used was first developed by S. R. Bodner and his graduate students at the Technion in Haifa, Israel in 1982 for a rigid penetrator impacting armor.** Instead of writing a conservation of energy equation or a force equilibrium equation, they wrote an energy rate equation. The rate at which kinetic energy leaves the penetrator and attached effective target mass must equal the rate at which energy is dissipated by strain energy, frictional effects, shear along boundaries and convective inertial effects. As will be apparent in discussions of derivations, this rate equation is equivalent to Newton's equation of motion, except some parameters representing the extent of a dynamic plastic flow field must be obtained by differentiating some of the

*Massianica, Frank, Ballistic Technology of Lightweight Armors, AMMRC-Tr-76-15, 1976 (confidential).

**M. Ravid and S. R. Bodner, "Dynamic Perforation of Viscoplastic Plates by Rigid Projectiles," Int. J. Engng. Sc., Vol. 21, No. 6, pp. 577-591, 1983.

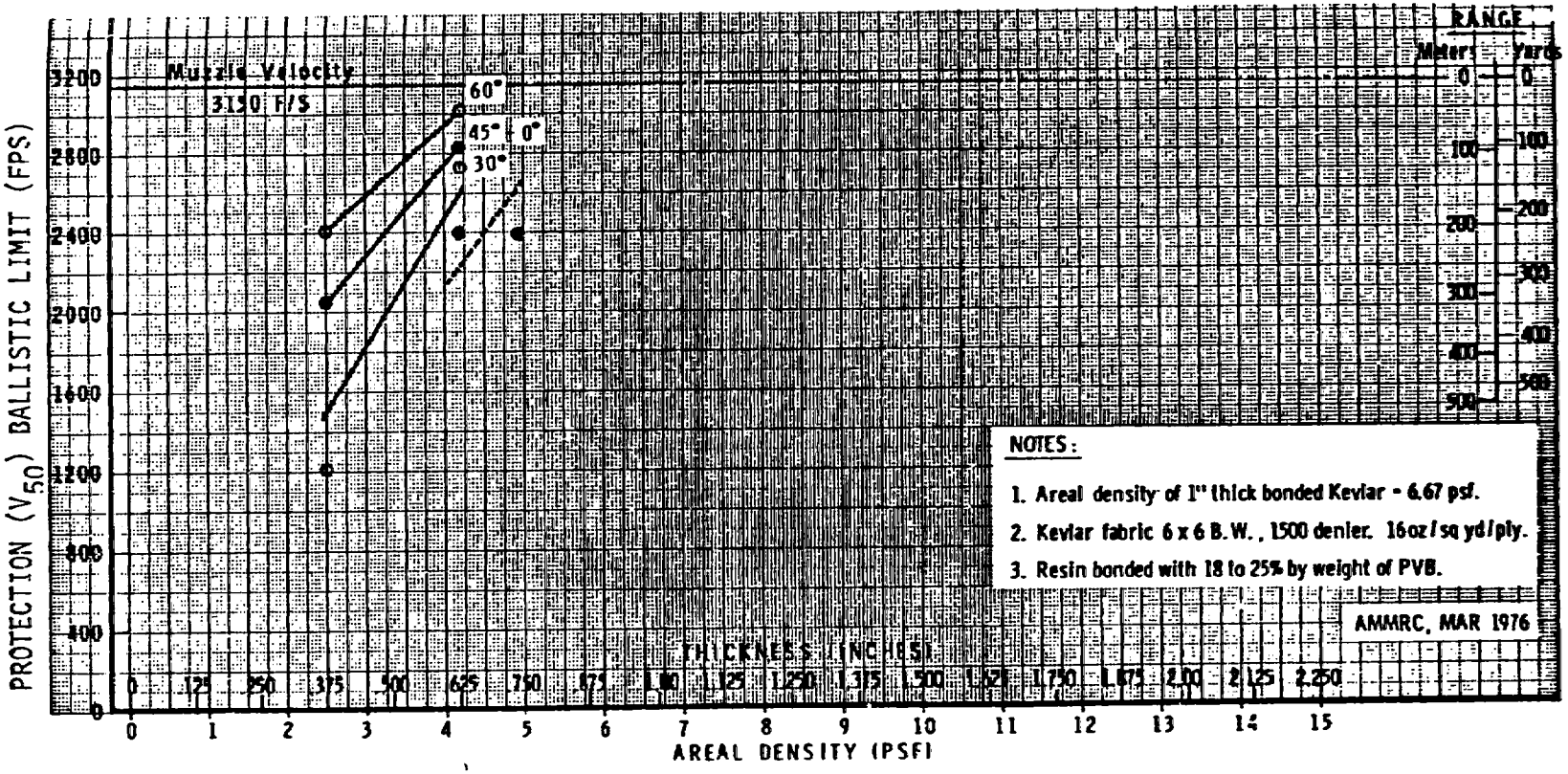

Figure 8. Protection Provided by Bonded Kevlar Fabric
Against 5.56mm Ball M193 Ammunition
Army Materials and Mechanics Research Center

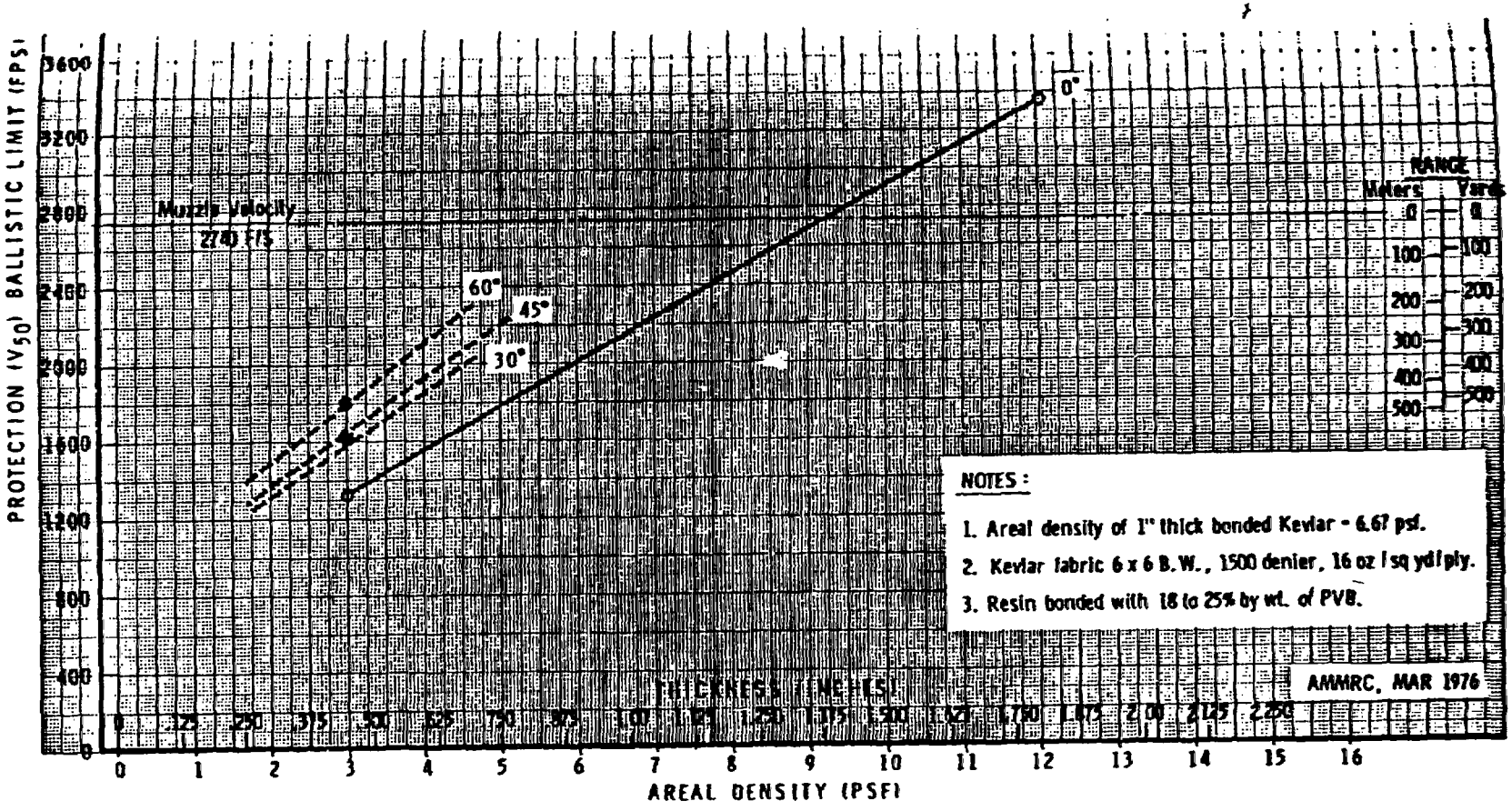

Figure 9. Protection Provided by Bonded Kevlar Fabric
Against 7.62mm Ball M80 Ammunition
Army Materials and Mechanics Research Center

a dynamic plastic flow field must be obtained by differentiating some of the terms to minimize the external forces applied to the penetrator.

In addition, a second key earlier contribution, made by Bodner and other earlier graduate students*, was that projectile penetration goes through a series of stages. One-stage engineering penetration models are seldom adequate. In our analysis, for a plugging mode of failure, we use a six-stage penetration process. At first the nose must become embedded in the target. In thick plates, nose embedment and a subsequent second stage result in material being ejected from the front face of the target. The top two figures in Figure 10 illustrate this behavior. Eventually, as the depth of penetration grows larger (stage 3), material is no longer ejected from any target face, and the penetration process becomes a cavity expansion process. As the penetration process increases, the plastic flow field ahead of the penetrator intersects the rear face of the armor, and a bulge begins to form. The stage 4 bulge grows larger until the ultimate strain is reached, and a plug in stage 5 of Figure 10 is ejected. Finally, in stage 6, the plug is ejected and the penetrator begins to emerge.

Whenever the armor is thin, the plastic flow field ahead of the penetrator will intersect the rear surface of the armor before the nose is fully embedded. Under this condition a stage 4 type bulge will occur which will lead to petaling of the armor when the ultimate strain is exceeded in stage 4. As soon as the petal begins to form, the armor is breeched. This second sequence of events can occur, and is referred to as a petaling mode in the sequence of events as opposed to a plugging mode.

To understand how this analysis is derived, consider a rigid penetrator in a stage 2 flow field as shown in Figure 11. In Figure 11 a plastic flow field extends out a distance NR from the focal point for the nose of a penetrator of radius R. This assumption basically states that a plastic disturbance extends out a uniform distance of (N-1)R from the surface of a penetrator with a hemispherical nose. Two zones are seen in this flow field, zones 1 and 2. Relative to the target itself the velocity V_{I-II} comes from conservation of the mass flow rate:

---

*V. Awerbuch and S. R. Bodner, "Analysis of the Mechanics of Perforation of Projectiles in Metallic Plates," Int. J. Solids Structures, Vol. 10, pp. 671-684, 1974.

Stage 1 - Initial Penetration

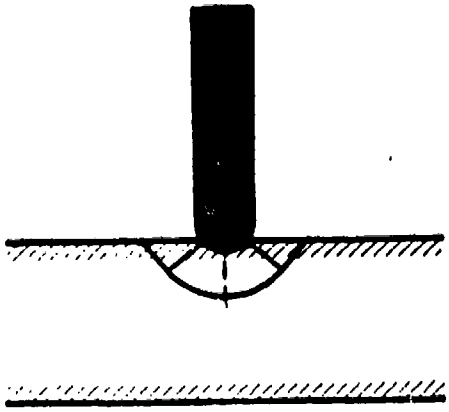

Stage 2 - Front Face Ejection of Material

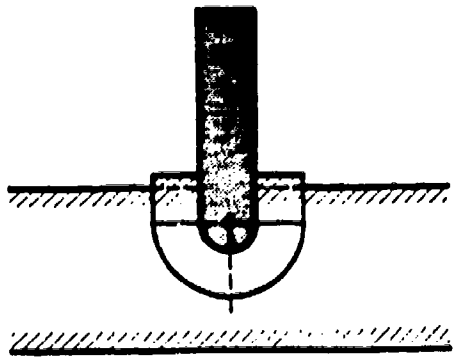

Stage 3 - Quasi Steady State Penetration

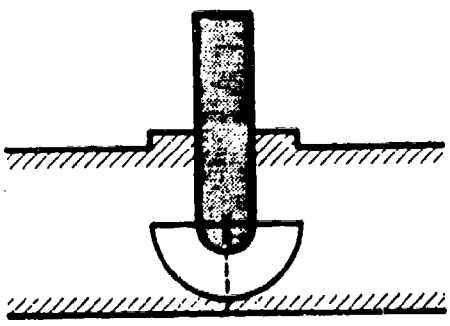

Stage 4 - Back Face Bulge Formation

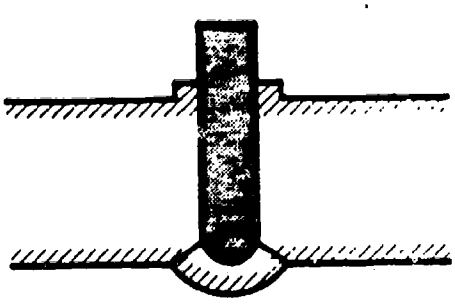

Stage 5 - Plug Ejection

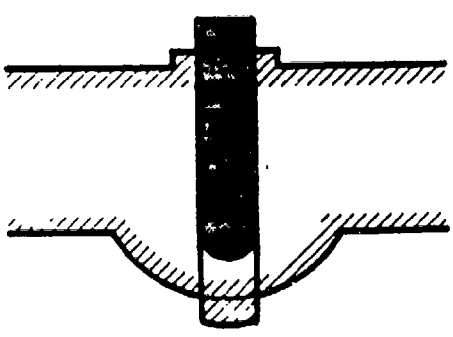

Stage 6 - Projectile Ejection

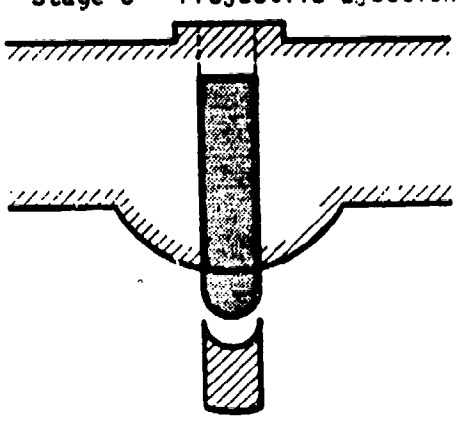

Figure 10. Stages in Long Rod Penetrator Perforation of Thick Target

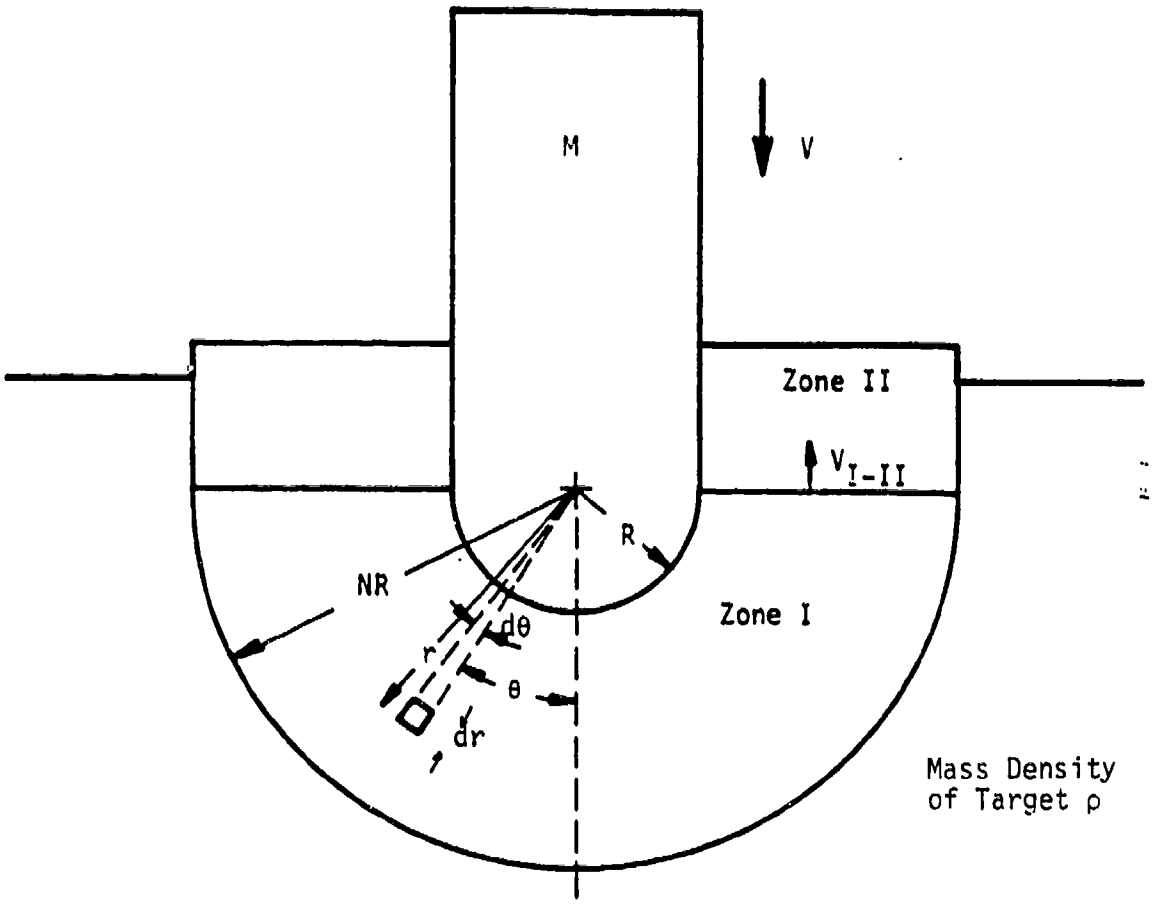

Figure 11. Second Stage Flow Field

$$V(\pi R^2) = V_{I-II} (\pi N^2 R^2 - \pi R^2) \tag{1}$$

or

$$V_{I-II} = \frac{V}{(N^2-1)} \tag{2}$$

Relative to the penetrator, V_{I-II} is:

$$V_{I-II} = \frac{V}{(N^2-1)} + V = \frac{N^2 V}{(N^2-1)} \tag{3}$$

Now a self-consistent flow field velocity distribution can be determined. Relative to the penetrator, the radial V_r and angular V_θ velocities are:

In Zone I	In Zone II	
$V_\theta = \frac{N^2 V \sin\theta}{(N^2-1)}$	$V_z = \frac{N^2 V}{(N^2-1)}$	(4a)
$V_r = \frac{N^2 \left(\frac{R^2}{r^2} - 1\right) V \cos\theta}{(N^2-1)}$	$V_r = 0$	(4b)
$V_\phi = 0$	$V_\phi = 0$	(4c)

The velocities can be inspected relative to the flow field boundaries to see that these are correct. At $\theta = 0°$, $V_\theta = 0$ and at $\theta = 90°$, $V_\theta = V_{I-II}$. At $\theta = 0°$ and $r = NR$, $V_r = -V$; at $\theta = 0°$ and $r = R$, $V_r = 0$; and at $\theta = 90°$, $V_r = 0$. In zone II, the motion is rigid body movement with the top and bottom moving at the same velocity. All velocities are relative to a coordinate system attached to the penetrator.

Now that the velocity field has been obtained, everything follows algebratically. The first energy rate to be calculated is the strain energy rate $\dot{w}_v$. To do this the strain rate fields must be obtained from the velocity field by differentiation. The strain rates in zone I are:

$$\dot{\varepsilon}_{rr} = \frac{\partial V_r}{\partial r} = \frac{-2\ V\ N^2\ R^2\ \cos\theta}{(N^2-1)\ r^3} \tag{5a}$$

$$\dot{\varepsilon}_{\theta\theta} = \frac{1}{r}\frac{\partial V_\theta}{\partial \theta} + \frac{V_r}{r} = \frac{N^2\ R^2\ V\ \cos\theta}{(N^2-1)\ r^3} \tag{5b}$$

$$\dot{\varepsilon}_{\phi\phi} = \frac{1}{r\ \sin\theta}\frac{\partial V_\theta}{\partial \theta} + \frac{V_r}{r} + V_\theta\ \frac{\cot\theta}{r} = \frac{N^2\ R^2\ V\ \cos\theta}{(N^2-1)\ r^3} \tag{5c}$$

$$\dot{\varepsilon}_{r\theta} = \frac{1}{2r}\frac{\partial V_r}{\partial \theta} - \frac{V_\theta}{2r} + \frac{\partial V_\theta}{2\partial r} = \frac{-\ N^2\ R^2\ V\ \cos\theta}{2\ (N^2-1)\ r^3} \tag{5d}$$

In zone II, rigid body motion results so that

$$\dot{\varepsilon}_{rr} = \dot{\varepsilon}_{zz} = \dot{\varepsilon}_{\theta\theta} = \dot{\varepsilon}_{r\theta} = 0 \tag{6}$$

The differential volume in zone I is:

$$dV_N = 2\ \pi\ r^2\ \sin\theta\ d\ r\ d\theta \tag{7}$$

Strain energy rate $\dot{w}_v$ in the plastic flow field is given by:

$$\dot{w}_v = \int_{v_N} \sigma_{ij}\ \dot{\varepsilon}_{ij}\ dV_N \tag{8}$$

which is:

$$\dot{w}_v = \int\int \left[\sigma\ (\dot{\varepsilon}_{rr} + \dot{\varepsilon}_{\theta\theta} + \dot{\varepsilon}_{\phi\phi}) + \frac{\sigma}{\sqrt{3}}\ (2\ \dot{\varepsilon}_{r\theta})\right] dV_N \tag{9}$$

After substituting Equations (5) and (7) into equation (9) and integrating one obtains:

$$\dot{w}_v = 2\ \pi\ \sigma\ V\ R^2\ \left(2.072\ \frac{N^2\ \ell n\ N}{(N^2-1)}\right) \tag{10}$$

There is no $\dot{w}_v$ in zone II because the $\dot{\varepsilon}$'s are zero.

Around the nose and over the embedded length of the penetrator there is a frictional shear energy rate $\dot{w}_f$. This $\dot{w}_f$ is given by:

$$\dot{w}_f = \int_A \tau_i \mid \Delta V_i \mid dA \tag{11}$$

where Δv_i is the velocity of one surface relative to the other and dA is the differential area of the interface. If τ is assumed to be $\mu\sigma$, where μ is a coefficient of friction, the friction energy rate is:

$$\dot{w}_f = \int_o^{\pi/2} \mu\sigma \frac{N^2}{(N^2-1)} V \sin\theta \, 2\pi R^2 \sin\theta \, d\theta + \mu\sigma \frac{N^2 V}{(N^2-1)} 2\pi R(Z-R) \tag{12}$$

or

$$\dot{w}_f = 2\pi\sigma V R^2 \left[\mu (Z/R - 0.2146) \frac{N^2}{(N^2-1)} \right] \tag{13}$$

In addition, a shear energy rate $\dot{w}_s$ occurs along boundaries of zones because they move relative to one another. The quantity $\dot{w}_s$ is given by the same general equation as $\dot{w}_f$, equation (11). In stage 2, $\dot{w}_s$ is given by:

$$\dot{w}_s = \frac{\sigma}{\sqrt{3}} \int_o^{\pi/2} \frac{V \sin\theta}{(N^2-1)} 2\pi N^2 R^2 \sin\theta \, d\theta + \frac{V}{(N^2-1)} 2\pi N R (Z-R) \tag{14}$$

The shear stress $\frac{\sigma}{\sqrt{3}}$, the Huber-Henke-Mises criteria, relates shear stress to normal yield stress. Completing the integration gives:

$$\dot{w}_s = 2\pi\sigma V R^2 \left[0.453 \frac{N^2}{(N^2-1)} + 0.5773 \frac{N}{(N^2-1)} \left(\frac{Z}{R} - 1\right) \right] \tag{15}$$

Before inertial energy rates can be determined, the velocity equations, equation (4), must be differentiated with respect to time to obtain accelerations. In zone I, the accelerations are

$$\frac{dV_r}{dt} = \frac{N^2\left(\frac{R^2}{r^2} - 1\right)}{(N^2-1)} \cos\theta\, \dot{V} - \frac{N^4\left(\frac{R^2}{r^2} - 1\right) \sin^2\theta\, V^2}{(N^2-1)\, r} - \frac{2N^4\left(\frac{R^4}{r^4} - \frac{R^2}{r^2}\right) \cos^2\theta\, V^2}{(N^2-1)^2\, r} \qquad (16a)$$

$$\frac{dV_\theta}{dt} = \frac{N^2 \sin\theta}{(N^2-1)} \dot{V} + \frac{N^4\, V^2 \sin(2\theta)}{2(N^2-1)^2\, r} \qquad (16b)$$

$$\frac{dV_z}{\partial t} = \frac{N^2}{(N^2-1)} \dot{V} \qquad (16c)$$

Notice that two types of acceleration terms exist: those with $\dot{V}$ in them and those with $\frac{V^2}{r}$ in them. This means that two different types of inertial energy rate terms will exist. The convective inertial terms $\dot{w}_k$ are obtained by using only those acceleration terms with $\frac{V^2}{r}$ in equation (16). The dynamic acceleration terms $\dot{w}_d$ are obtained by using only the $\dot{v}$ acceleration terms in equation (16). No matter which type of inertial energy rate is being computed, the inertial energy rate is given by:

$$\dot{w}_I = \int_{V_N} \frac{d}{dt}\left(\frac{\rho\, V_i^2}{2}\right) dV_N = \rho \int_{V_N} V_i \cdot \dot{V}_i\, dV_N \qquad (17)$$

Substituting the velocity and acceleration fields into equation (17) gives for the convective energy rate $\dot{w}_k$:

$$\dot{w}_k = \rho \int_0^{\pi/2} \int_R^{NR} - \frac{N^4\left(\frac{R^2}{r^2} - 1\right) \sin^2\theta\, V^2}{(N^2-1)\, r} + \frac{2N^4\left(\frac{R^4}{r^4} - \frac{R^2}{r^2}\right) \cos^2\theta\, V^2}{(N^2-1)^2\, r} \cdot$$

$$\frac{N^2\left(\frac{R^2}{r^2} - 1\right) V \cos\theta}{(N^2-1)} \left(2\pi r^2 \sin^2\theta\, d\theta\, dr\right)$$

$$+ \rho \int_0^{\pi/2} \int_R^{NR} \frac{N^4\, V^2 \sin(2\theta)}{2\,(N^2-1)2\, r} \quad \frac{N^2\, V \sin\theta}{(N^2-1)} \left(2\pi r^2 \sin^2\theta\, d\theta\, dr\right) \qquad (18)$$

or

$$\dot{w}_k = 2\,\pi\,\rho\,V^3\,R^2\left[\frac{N^2(2N^2-1)}{8(N^2-1)}\right] \tag{19}$$

The dynamic acceleration energy rate $\dot{w}_d$ is:

$$\dot{w}_d = \rho\int_o^{\pi/2}\int_R^{NR}\frac{N^2\left(\frac{R^2}{r^2}-1\right)}{(N^2-1)}\cos\theta\,\dot{V}\;\frac{N^2\left(\frac{R^2}{r^2}-1\right)V\cos\theta}{(N^2-1)}\,(2\pi\,r^2\sin^2\theta\,d\theta\,dr)$$

$$+\,\rho\int_o^{\pi/2}\int_R^{NR}\frac{N^2\sin\theta}{(N^2-1)}\,\dot{V}\;\frac{N^2\,V\sin\theta}{(N^2-1)}\,(2\pi\,r^2\sin^2\theta\,d\theta\,dr)$$

$$+\,\rho\;\frac{N^2\,\dot{V}}{(N^2-1)}\;\frac{N^2\,V}{(N^2-1)}\left[\pi\,R^2(N^2-1)(Z-R)\right] \tag{20}$$

or

$$\dot{w}_d = 2\pi\,\rho\,V\,\dot{V}\,R^2\;\frac{N^3(N^4-6N^2+8N-3)}{9(N^2-1)^2}+\frac{2N^4(N^3-1)}{9(N^2-1)^2}+\frac{N^4(Z/R-1)}{2(N^2-1)} \tag{21}$$

The final energy rate term is the energy rate in the rigid penetrator. The penetrator's inertial energy rate term $\dot{w}_p$ is:

$$\dot{w}_p = \frac{d}{dt}\left(\frac{m}{2}V^2\right) = m\,V\,\dot{V} \tag{22}$$

Now all the energy rate terms have been derived for stage 2 in the penetration process. Notice that of all the energy rate terms, only equations (21) and (22) have $V\,\dot{V}$ in them. Equation (21) is the local dynamic acceleration which adds an effective mass of target material to the mass of the penetrator. If energy rates are equated, the energy rate loss from the sum of

equations (21) and (22) must go into $\dot{w}_s + \dot{w}_k + \dot{w}_f + \dot{w}_v$. Mathematically this process is:

$$\left[M + 2\pi\,\rho\,R^3\left\{\frac{N^3(N^4 - 6N^2 + 8N - 3) + 2N^4(N^3-1)}{9(N^2-1)^2}\right\}\right]\frac{dV}{dt} =$$

$$-4.144\pi\,\frac{N^2\,\ell n\,N}{(N^2-1)}\,\sigma\,R^2 - 2\pi\,\mu\left(\frac{Z}{R} - 0.2146\right)\frac{N^2}{(N^2-1)}\,\sigma\,R^2$$

$$-\left[0.4534\,\frac{N^2}{(N^2-1)} + 0.5773\,\frac{N}{(N^2-1)}\left(\frac{Z}{R} - 1\right)\right]2\pi\,\sigma\,R^2$$

$$-\left[\frac{\pi}{4}\,\frac{N^2(2N^2-1)}{(N^2-1)^2}\right]\rho\,R^2\,V^2 \qquad (23)$$

By substituting $V\,\frac{dV}{dz}$ for $\frac{dV}{dt}$, equation (23) could be solved for dV using incremental dz steps if the extent of the plastic flow field given by N could be obtained. Equation (23), obtained by balancing energy rates is Newton's equation of motion. The left-hand side is the total acting mass (penetrator and effective target mass) times the acceleration. All of the $\dot{w}_v + \dot{w}_f + \dot{w}_s + \dot{w}_k$ terms on the right-hand side give the external forces acting on the penetrator. This point is a very important statement.

To obtain N so that the equation of motion can be solved, we differentiate the right-hand side of equation (23) only with respect to N and set the result equal to zero. This process says that the extent of the plastic flow field will be such that the transient external forces on the projectile are minimized. In other words, the projectile follows the path of least resistance. Differentiation thus gives a second relationship.

$$\frac{\partial F_{ext}}{\partial N} = 0 = -4.144\,\ell n\,N + 2.9788(N^2-1) - 0.8\left(\frac{Z}{R} - 0.2146\right) - 0.9068\,N^2$$

$$- 1.154\left(\frac{Z}{R} - 1\right)N + 0.5773\left(\frac{Z}{R} - 1\right)\left(N - \frac{1}{N}\right) - \frac{(3N^2-1)}{4(N^2-1)}\left(\frac{\rho\,V^2}{\sigma}\right) \qquad (24)$$

For specific values of Z/R and $\frac{\rho V^2}{\sigma}$, equation (24) can be solved for N. After N is obtained dV is obtained from equation (23). Solving equations (23) and (24) are iterative procedures. Equation (24) is for the extent of the plastic flow field; equation (23) is the equation of motion.

Similar mathematical procedures were followed for all of the stages. If the equations for all stages were presented, more than 200 equations would be presented. By presenting the mathematics in stage 2, the reader sees the processes which are considered. Those wishing complete details and derivations for all stages should obtain SwRI's report for TACOM when it appears.*

All threshold penetration velocities were obtained using the same procedure. If a target was multi-layered, as with the aluminum munition in the fiberglass shipping container, the residual velocity of the stub exiting the fiberglass became the input velocity into the aluminum. Various impact velocities were tried in a trial and error procedure until the velocity for just penetrating the aluminum was within 0.1 ft/sec of a velocity which does not penetrate. Finally the threshold velocity was obtained by averaging these two velocities.

Whenever an equivalent thickness of steel was obtained, various mild steel thicknesses of armor were tried for that radius of stub and impact velocity until a thickness was obtained for penetrating and another for not penetrating which were within 0.01 inches of each other. Hence, all plots of stub radius versus impact velocity or equivalent thickness of mild steel versus stub radius come from a sequence of trial and error runs.

The advantage of analysis procedure relative to hydrocode is that only two equations must be solved at each time step rather than hundreds, or even thousands, of equations as in any numerical hydrocode. The number of equations is decreased by using this engineering analysis technique. Nevertheless, essentially all physical processes except strain rate effects nad penetrator erosion are included. That the analysis can work is already demonstrated in Figure 7 for drop tests of lead blocks onto stubs.

A listing for the entire computer program will appear in SwRI's report for TACOM when it is approved for release by the sponsor.

---

*P. Westine, Development of an Engineering Computer Code for Eroding Projectile Penetration and Perforation of Armor, Contract DAA07-84-C-R120.

UNCLASSIFIED

SECURITY CLASSIFICATION OF THIS PAGE

REPORT DOCUMENTATION PAGE

1a. REPORT SECURITY CLASSIFICATION Unclassified	1b. RESTRICTIVE MARKINGS None AD897797
2a. SECURITY CLASSIFICATION AUTHORITY NA	3 DISTRIBUTION / AVAILABILITY OF REPORT Distribution Unlimited/Approved for Public Release AMCPEB-D
2b. DECLASSIFICATION / DOWNGRADING SCHEDULE NA	
4 PERFORMING ORGANIZATION REPORT NUMBER(S) 06-8461-003/004	5. MONITORING ORGANIZATION REPORT NUMBER(S) AMXTH-CD-TR-86058 Chemical Demilitarization
6a. NAME OF PERFORMING ORGANIZATION Southwest Research Institute 6b OFFICE SYMBOL (If applicable)	7a. NAME OF MONITORING ORGANIZATION U.S. Army Toxic and Hazardous Materials Agency
6c. ADDRESS (City, State, and ZIP Code) P. O. Drawer 28510 6220 Culebra Road San Antonio, Texas 78284	7b. ADDRESS (City, State, and ZIP Code) Aberdeen Proving Ground, MD 21010-5401
8a. NAME OF FUNDING / SPONSORING ORGANIZATION H&R Technical Associates, Inc. 8b. OFFICE SYMBOL (If applicable)	9. PROCUREMENT INSTRUMENT IDENTIFICATION NUMBER
8c. ADDRESS (City, State, and ZIP Code) P. O. Box 215 Oak Ridge, Tennessee 37831	10. SOURCE OF FUNDING NUMBERS PROGRAM ELEMENT NO. / PROJECT NO. / TASK NO. / WORK UNIT ACCESSION NO.

11 TITLE (Include Security Classification)
Stub Penetration in Chemical Munition Shipment

12 PERSONAL AUTHOR(S)
Westine, Peter S.

13a. TYPE OF REPORT	13b. TIME COVERED	14. DATE OF REPORT (Year, Month, Day)	15. PAGE COUNT
Final	FROM _____ TO _____	85.05	24

16. SUPPLEMENTARY NOTATION

17. COSATI CODES			18. SUBJECT TERMS (Continue on reverse if necessary and identify by block number)
FIELD	GROUP	SUB-GROUP	
15	02		Transportation Accident, Stub Penetration, Chemical Munition Container, M55

19. ABSTRACT (Continue on reverse if necessary and identify by block number)

The M55 warhead carries a chemical agent which must be protected from accidental puncture in a shipment or handling accident. This report presents results from computer runs calculating the threshold impact velocity if a pallet of munitions or a protective package containing several pallets were to be dropped onto rigid stubs of different radii. Calculations were made for three separate cases. Case 1 involved stub penetration of a fiberglass shipping container and then the aluminum walls of the round. Case 2 added an extra layer of protection so that wooden two by fours had to be penetrated before the shipping container and munition walls were penetrated. Case 3 was an independent scenario involving puncture of a CAMPACT shipping container loaded on a flat bed railroad car or highway vehicle.

The computer code used to make all computation is a dynamic plasticity, multi-penetration stage, one just developed by SwRI for the U. S. Army Tank Automotive Command. Some comparisons are presented in which this code predicts experimentally observed penetrations to demonstrate the validity of its use in this study.

20 DISTRIBUTION / AVAILABILITY OF ABSTRACT ☐ UNCLASSIFIED/UNLIMITED ☒ SAME AS RPT. ☐ DTIC USERS	21. ABSTRACT SECURITY CLASSIFICATION Unclassified
22a NAME OF RESPONSIBLE INDIVIDUAL CPT Kevin J. Flamm	22b. TELEPHONE (Include Area Code) (301) 671-2424 22c. OFFICE SYMBOL AMXTH-CD-L

DD FORM 1473, 84 MAR 83 APR edition may be used until exhausted. All other editions are obsolete.

SECURITY CLASSIFICATION OF THIS PAGE

UNCLASSIFIED